

NONEQUILIBRIUM PARTON DYNAMICS IN THE STRONGLY INTERACTING QGP

W. Cassing^a, E. L. Bratkovskaya^b

^a Institut für Theoretische Physik, Justus-Liebig-Universität Giessen, Germany

^b Institut für Theoretische Physik, Goethe-Universität Frankfurt am Main, Germany

The dynamics of partons, hadrons and strings in relativistic nucleus–nucleus collisions is analyzed within the novel Parton-Hadron-String Dynamics (PHSD) transport approach, which is based on a dynamical quasiparticle model for partons (DQPM) matched to reproduce recent lattice-QCD results — including the partonic equation of state — in thermodynamic equilibrium. The transition from partonic to hadronic degrees of freedom is described by covariant transition rates for the fusion of quark–antiquark pairs or three quarks (antiquarks), respectively, obeying flavor current conservation, color neutrality as well as energy-momentum conservation. Since the dynamical quarks and antiquarks become very massive close to the phase transition, the formed resonant «pre-hadronic» color-dipole states ($q\bar{q}$ or qqq) are of high invariant mass, too, and sequentially decay to the ground-state meson and baryon octets increasing the total entropy. When applying the PHSD approach to Pb + Pb collisions at 158A GeV, we find a significant effect of the partonic phase on the production of multistrange antibaryons due to a slightly enhanced $s\bar{s}$ pair production from massive time-like gluon decay and a larger formation of antibaryons in the hadronization process.

PACS: 25.70.Gh; 12.38.Mh

The «Big Bang» scenario implies that in the first microseconds of the universe the entire state has emerged from a partonic system of quarks, antiquarks and gluons — a quark–gluon plasma (QGP) — to color neutral hadronic matter consisting of interacting hadronic states (and resonances) in which the partonic degrees of freedom are confined. The nature of confinement and the dynamics of this phase transition has motivated a large community for several decades and is still an outstanding question of today’s physics. Early concepts of the QGP were guided by the idea of a weakly interacting system of partons which might be described by perturbative QCD (pQCD). However, experimental observations at the Relativistic Heavy Ion Collider (RHIC) indicated that the new medium created in ultrarelativistic Au + Au collisions is interacting more strongly than hadronic matter and consequently this concept had to be severely questioned. Moreover, in line with theoretical studies in [1–3], the medium showed phenomena of an almost perfect liquid of partons [4, 5] as extracted from the strong radial expansion and the scaling of elliptic flow $v_2(p_T)$ of mesons and baryons with the number of constituent quarks and antiquarks [4].

The question about the properties of this (nonperturbative) QGP liquid is discussed controversially in the literature, and dynamical concepts describing the formation of color neutral hadrons from colored partons are scarce. A fundamental issue for hadronization models is the conservation of 4-momentum as well as the entropy problem because by fusion/coalescence of massless (or low constituent mass) partons to color neutral bound states of low invariant mass (e.g., pions) the number of degrees of freedom and thus the total entropy is reduced

in the hadronization process [6–8]. This problem — a violation of the second law of thermodynamics as well as the conservation of four-momentum and flavor currents — has been addressed in [9] on the basis of the DQPM employing covariant transition rates for the fusion of «massive» quarks and antiquarks to color neutral hadronic resonances or strings. In fact, the dynamical studies for an expanding partonic fireball in [9] suggest that the latter problems have come to a practical solution.

A consistent dynamical approach — valid also for strongly interacting systems — can be formulated on the basis of Kadanoff–Baym (KB) equations [10] or off-shell transport equations in phase-space representation, respectively [10–12]. In the KB theory the field quanta are described in terms of dressed propagators with complex self-energies. Whereas the real part of the self-energies can be related to mean-field potentials (of Lorentz scalar, vector or tensor type), the imaginary parts provide information about the lifetime and/or reaction rates of time-like «particles» [13]. Once the proper (complex) self-energies of the degrees of freedom are known, the time evolution of the system is fully governed by off-shell transport equations (as described in [10, 13]). The determination/extraction of complex self-energies for the partonic degrees of freedom has been performed before in [14, 15] by fitting lattice QCD (lQCD) «data» within the Dynamical QuasiParticle Model (DQPM). In fact, the DQPM allows for a simple and transparent interpretation of lattice QCD results for thermodynamic quantities as well as correlators and leads to effective strongly interacting partonic quasiparticles with broad spectral functions. For a review on off-shell transport theory and results from the DQPM, in comparison to lQCD, we refer the reader to [13].

Since the actual implementations in the PHSD transport approach have been presented in detail in [16], we here report again on the actual description of hadronization and present results for Pb + Pb collisions at SPS energies in comparison to experimental data from the NA49 collaboration.

1. HADRONIZATION IN PHSD

The hadronization, i.e., the transition from partonic to hadronic degrees of freedom, is described in PHSD by local covariant transition rates as introduced in [9], e.g., for $q + \bar{q}$ fusion to a meson m of four-momentum $p = (\omega, \mathbf{p})$ at space-time point $x = (t, \mathbf{x})$:

$$\begin{aligned} \frac{dN_m(x, p)}{d^4x d^4p} &= \text{Tr}_q \text{Tr}_{\bar{q}} \delta^4(p - p_q - p_{\bar{q}}) \delta^4\left(\frac{x_q + x_{\bar{q}}}{2} - x\right) \times \\ &\quad \times \omega_q \rho_q(p_q) \omega_{\bar{q}} \rho_{\bar{q}}(p_{\bar{q}}) |v_{q\bar{q}}|^2 W_m(x_q - x_{\bar{q}}, (p_q - p_{\bar{q}})/2) \times \\ &\quad \times N_q(x_q, p_q) N_{\bar{q}}(x_{\bar{q}}, p_{\bar{q}}) \delta(\text{flavor, color}). \end{aligned} \quad (1)$$

In Eq. (1) we have introduced the shorthand notation,

$$\text{Tr}_j = \sum_j \int d^4x_j \int \frac{d^4p_j}{(2\pi)^4}, \quad (2)$$

where \sum_j denotes a summation over discrete quantum numbers (spin, flavor, color); $N_j(x, p)$ is the phase-space density of parton j at space-time position x and four-momentum p . In Eq. (1) $\delta(\text{flavor, color})$ stands symbolically for the conservation of flavor quantum numbers as well

as color neutrality of the formed hadron m which can be viewed as a color-dipole or «pre-hadron». Furthermore, $v_{q\bar{q}}(\rho_p)$ is the effective quark–antiquark interaction from the DQPM (displayed in Fig. 10 of [15]) as a function of the local parton ($q + \bar{q} + g$) density ρ_p (or energy density). Furthermore, $W_m(x, p)$ is the dimensionless phase-space distribution of the formed «pre-hadron», i.e.,

$$W_m(\xi, p_\xi) = \exp\left(\frac{\xi^2}{2b^2}\right) \exp\left[2b^2\left(p_\xi^2 - \frac{(M_q - M_{\bar{q}})^2}{4}\right)\right] \quad (3)$$

with $\xi = x_1 - x_2 = x_q - x_{\bar{q}}$ and $p_\xi = (p_1 - p_2)/2 = (p_q - p_{\bar{q}})/2$. The width parameter b is fixed by $\sqrt{\langle r^2 \rangle} = b = 0.66$ fm (in the rest frame) which corresponds to an average rms radius of mesons. We note that the expression (3) corresponds to the limit of independent harmonic oscillator states and that the final hadron-formation rates are approximately independent of the parameter b within reasonable variations. By construction the quantity (3) is Lorentz-invariant; in the limit of instantaneous «hadron formation», i.e., $\xi^0 = 0$, it provides a Gaussian dropping in the relative distance squared $(\mathbf{r}_1 - \mathbf{r}_2)^2$. The four-momentum dependence reads explicitly (except for a factor $1/2$)

$$(E_1 - E_2)^2 - (\mathbf{p}_1 - \mathbf{p}_2)^2 - (M_1 - M_2)^2 \leq 0 \quad (4)$$

and leads to a negative argument of the second exponential in (3) favoring the fusion of partons with low relative momenta $p_q - p_{\bar{q}} = p_1 - p_2$.

Related transition rates (to Eq. (1)) are defined for the fusion of three off-shell quarks ($q_1 + q_2 + q_3 \leftrightarrow B$) to color neutral baryonic (B or \bar{B}) resonances of finite width (or strings) fulfilling energy and momentum conservation as well as flavor current conservation using Jacobi coordinates (cf. [16]).

On the hadronic side the PHSD transport approach includes explicitly the baryon octet and decouplet, the 0^- - and 1^- -meson nonets as well as selected higher resonances as in HSD [17]. Hadrons of higher masses (> 1.5 GeV in case of baryons and > 1.3 GeV in case of mesons) are treated as «strings» (color dipoles) that decay to the known (low-mass) hadrons according to the JETSET algorithm [18]. We discard an explicit recapitulation of the string decay and refer the reader to the original work [18] or [19].

2. APPLICATION TO NUCLEUS–NUCLEUS COLLISIONS

In this Section we employ the PHSD approach to nucleus–nucleus collisions at moderate relativistic energies, i.e., at SPS energies where our approximations are expected to work. Note that at RHIC or LHC energies other initial conditions (e.g., a color-glass condensate [20]) might be necessary. Since this is a slightly different subject we here restrict ourselves to bombarding energies below $160A$ GeV where such problems/questions are expected to be not relevant.

We continue with a consideration of energy partitions in order to map out the fraction of partonic energy in time for relativistic nucleus–nucleus collisions. In Fig. 1, *a* we show the energy balance for a central (impact parameter $b = 1$ fm) reaction of Pb + Pb at $158A$ GeV, i.e., at the top SPS energy. The total energy E_{tot} (upper line) — which at $t = 0$ is given by the energy of the colliding nuclei in the cms — is conserved throughout the reaction, i.e., in

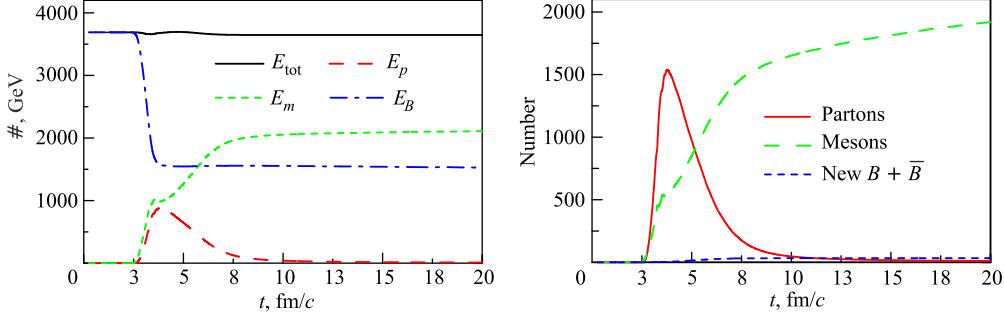


Fig. 1. *a)* The total energy E_{tot} (upper solid line) for central ($b = 1$ fm) collisions of Pb+Pb at 158A GeV. The long-dashed line shows the energy contributions E_p from partons, while the short-dashed line displays the energy contribution from mesons E_m (including «unformed mesons» in strings). The dash-dotted line is the contribution of baryons (and antibaryons) E_B ; the difference between the initial baryonic energy $E_B(t = 0)$ and final baryonic energy $E_B(t \rightarrow \infty)$ gives the energy that is converted during the heavy-ion collision to final mesonic states. *b)* The number of produced partons (solid line), mesons (long-dashed line) and newly produced baryon + antibaryons (short-dashed line) as a function of time for Pb+Pb at 158A GeV (for $b = 1$ fm). Note that the number of mesons still increases for $t > 20$ fm/c due to the decay of vector mesons

the partonic and hadronization phase as well as in the hadronic phase. Whereas in the first ~ 3 fm/c the total energy is entirely contained in the impinging nucleons (including about 6 MeV per nucleon of binding energy), a rapid transition to partonic degrees of freedom is seen at $t \approx 3$ fm/c, i.e., when the nuclei have started to overlap and react. We recall that the transition time of the two Pb nuclei is about $2R_{\text{Pb}}/\gamma_{\text{cm}} \approx 1.5$ fm/c at the top SPS energy. During this time period about 60% of initial kinetic energy of nucleons is converted to partons (long-dashed line) and to mesons (short-dashed line) in the surface region («corona») of the colliding system. Note that in the «mesonic» energy E_m also «unformed mesons» — as fragments of the strings — are accounted for. The energy of residual baryons (including antibaryons) is shown in terms of the dash-dotted line and is almost constant for $t > 5$ fm/c implying that the various final-state interactions do not show up significantly in the energy fractions. The partonic phase — in a limited space-time region — approximately ends for $t > 9$ fm/c which means that the further time evolution of the system is essentially described by hadronic interactions (HSD). Note that a sizeable fraction of energy is asymptotically still contained in the baryons. Since the baryon-rest masses amount to an energy of about 449 GeV (including newly produced $B\bar{B}$ pairs) this implies that full stopping is not achieved in central Pb+Pb collisions at 158A GeV. We note in passing that the net proton rapidity distributions are well described in the SPS energy regime from 40 to 158A GeV in comparison to the NA49 data [16].

Let us have a closer look at the «particle» composition in time for this reaction. We concentrate on those species that carry the energy transferred during the collision to new degrees of freedom. In this respect we display in Fig. 1, *b* the number of produced partons (solid line), mesons (long-dashed line) and newly produced baryons + antibaryons (short-dashed line) as a function of time for the same reaction as before. We recall that the initial number of nucleons is 416 in this case. Slightly more than 1500 partons are produced

during the passage time of the nuclei which disappear practically after 9 fm/c and essentially form mesons. The number of newly produced $B + \bar{B}$ pairs is small at this energy, but its flavor decomposition is quite interesting. An essential point here is that the number of final hadronic states is larger than the number of partons; i.e., there is a production of entropy in the hadronization process as pointed out before in [9]. This implies that in PHSD the second law of thermodynamics is not violated in the hadronization process!

As found in [16], the impact of the partonic degrees of freedom in PHSD on the longitudinal rapidity distribution of protons, pions and kaons is only small in central Pb + Pb collisions at SPS energies from 40 to 158A GeV. More sensitive experimental information is provided by the differential abundancies of baryons and antibaryons with strangeness. However, as discussed in [16] — and shown in Fig. 2 — even the double strange baryons (Ξ^- , Ξ^0) exhibit no significant enhancement from the partonic phase relative to HSD. This situation changes for double antistrange baryons: in Fig. 3 we present the PHSD rapidity spectra of

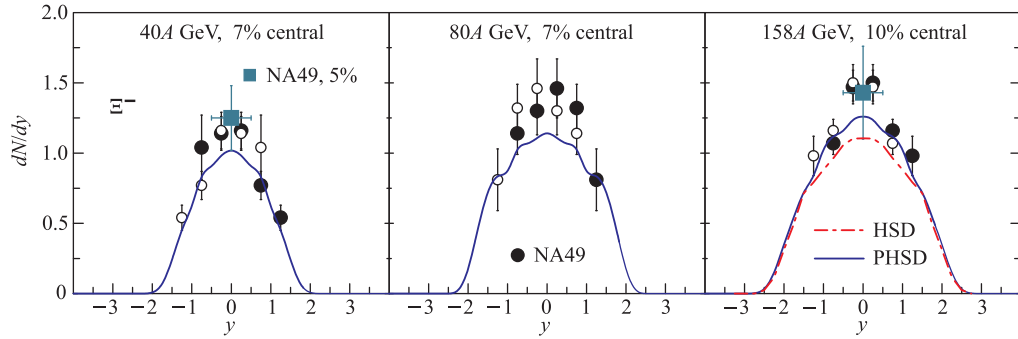


Fig. 2. The Ξ^- rapidity distributions for 7% central Pb + Pb collisions at 40, 80 and 10% central Pb + Pb collisions at 158A GeV from PHSD (thick solid lines) in comparison to the distribution from HSD (dash-dotted line for 158A GeV) and the experimental data (circles) from the NA49 collaboration [22] (the open circles correspond to data points reflected at midrapidity). The full square at $y = 0$ corresponds to the recent 5% central data point from [21]

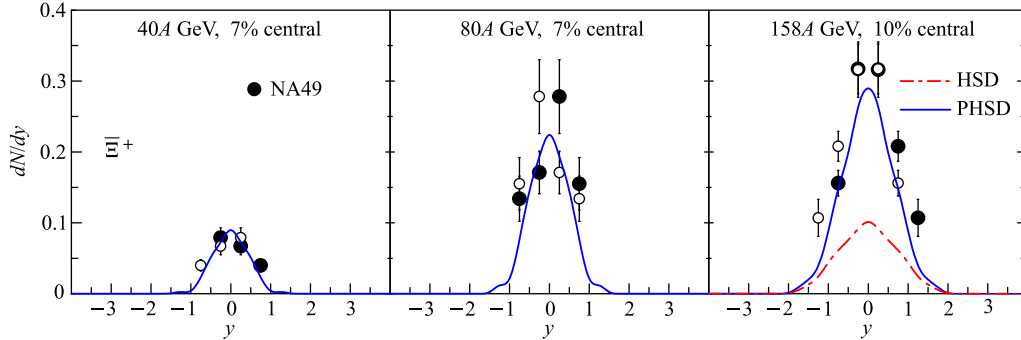


Fig. 3. The Ξ^+ rapidity distributions for central Pb + Pb collisions at 40, 80 and 10% central Pb + Pb collisions at 158A GeV from PHSD (thick solid lines) in comparison to the distribution from HSD (dash-dotted line for 158A GeV) and the experimental data (circles) from the NA49 collaboration [22] (the open circles correspond to data points reflected at midrapidity)

$\bar{\Xi}^+$ for 7 or 10% central reactions of Pb + Pb at 40, 80 and 158A GeV by the solid lines, respectively. Indeed, the PHSD description of the data now is sufficiently good contrary to the HSD calculations at 158A GeV (dash-dotted line) which underestimate the data by a factor of about three. This observation points towards a partonic origin but needs further examination.

3. SUMMARY

In this contribution we have addressed relativistic collisions of Pb + Pb at SPS energies in the PHSD approach which includes explicit partonic degrees of freedom as well as dynamical local transition rates from partons to hadrons (1). The hadronization process conserves four-momentum and all flavor currents and slightly increases the total entropy since the «fusion» of rather massive partons dominantly leads to the formation of color neutral strings or resonances that decay microcanonically to lower mass hadrons. Since this dynamical hadronization process increases the total entropy, the second law of thermodynamics is not violated (as is the case for simple coalescence models incorporating massless partons).

The PHSD approach has been also applied to nucleus–nucleus collisions from 40 to 160A GeV in order to explore the space-time regions of «partonic matter» [16]. We have found that even central collisions at the top SPS energy of $\sim 158A$ GeV show a large fraction of nonpartonic, i.e., hadronic or string-like matter, which can be viewed as a «hadronic corona». This finding implies that neither purely hadronic nor purely partonic «models» can be employed to extract physical conclusions in comparing model results with data. On the other hand — studying in detail Pb + Pb reactions at SPS energies in comparison to the data [16] — it is found that the partonic phase has only a very low impact on the longitudinal rapidity distributions of hadrons but a sizeable influence on the transverse-mass distribution of final kaons due to the partonic interactions. The most pronounced effect is seen on the production of multistrange antibaryons due to a slightly enhanced $s\bar{s}$ pair production in the partonic phase from massive time-like gluon decay and a more abundant formation of strange antibaryons in the hadronization process. This enhanced formation of strange antibaryons in central Pb + Pb collisions at SPS energies by hadronization supports the early suggestion by Braun–Munzinger and Stachel [23, 24] in the statistical hadronization model — which describes well particle ratios from AGS to RHIC energies.

Some note of caution has to be stated here with respect to applications of PHSD at FAIR energies (5–40A GeV) since the partonic equation of state employed so far describes a crossover transition between the hadronic and partonic phase, while at lower SPS and FAIR energies a first-order phase transition and the appearance of a critical point in the QCD phase diagram are expected [25]. Such phenomena may not be described by the present realization of PHSD but need subtle extensions.

REFERENCES

1. Shuryak E. // Prog. Part. Nucl. Phys. 2004. V. 53. P. 273.
2. Thoma M. H. // J. Phys. G. 2005. V. 31. P. L7; Nucl. Phys. A. 2006. V. 774. P. 307.
3. Peshier A., Cassing W. // Phys. Rev. Lett. 2005. V. 94. P. 172301.

4. *Arsene I. et al. // Nucl. Phys. A. 2005. V. 757. P. 1;*
Back B. B. et al. // Ibid. P. 28;
Adams J. et al. // Ibid. P. 102;
Adcox K. et al. // Ibid. P. 184.
5. *Hirano T., Gyulassy M. // Nucl. Phys. A. 2006. V. 769. P. 71.*
6. *Hwa R. C., Yang C. B. // Phys. Rev. C. 2003. V. 67. P. 034902;*
Greco V., Ko C. M., Levai P. // Phys. Rev. Lett. 2003. V. 90. P. 202302.
7. *Fries R. J. et al. // Ibid. P. 202303.*
8. *Lin Z.-W. et al. // Phys. Rev. C. 2005. V. 72. P. 064901.*
9. *Cassing W., Bratkovskaya E. L. // Phys. Rev. C. 2008. V. 78. P. 034919.*
10. *Juchem S., Cassing W., Greiner C. // Phys. Rev. D. 2004. V. 69. P. 025006; Nucl. Phys. A. 2004. V. 743. P. 92.*
11. *Cassing W., Juchem S. // Nucl. Phys. A. 2000. V. 665. P. 377; V. 672. P. 417.*
12. *Ivanov Y. B., Knoll J., Voskresensky D. N. // Ibid. P. 313.*
13. *Cassing W. // Eur. Phys. J. ST. 2009. V. 168. P. 3.*
14. *Cassing W. // Nucl. Phys. A. 2007. V. 791. P. 365.*
15. *Cassing W. // Ibid. V. 795. P. 70.*
16. *Cassing W., Bratkovskaya E. L. // Nucl. Phys. A. 2009. V. 831. P. 215.*
17. *Cassing W., Bratkovskaya E. L. // Phys. Rep. 1999. V. 308. P. 65.*
18. *Bengtsson H.-U., Sjöstrand T. // Comp. Phys. Commun. 1987. V. 46. P. 43.*
19. *Falter T. et al. // Phys. Rev. C. 2004. V. 70. P. 054609.*
20. *McLerran L. // Nucl. Phys. A. 2007. V. 787. P. 1; Intern. J. Mod. Phys. A. 2006. V. 21. P. 694.*
21. *Anticic T. et al. (NA49 Collab.) // Phys. Rev. C. 2009. V. 80. P. 034906.*
22. *Alt C. et al. (NA49 Collab.) // Phys. Rev. C. 2008. V. 78. P. 034918.*
23. *Braun-Munzinger P. et al. // Phys. Lett. B. 1996. V. 365. P. 1; 1999. V. 465. P. 15; 2001. V. 518. P. 41.*
24. *Andronic A., Braun-Munzinger P., Stachel J. // Nucl. Phys. A. 2006. V. 772. P. 167.*
25. *Senger P. et al. CBM Physics Book (in press).*